

**Note added after first publication:** this version of the Electronic Supplementary Information published on 16<sup>th</sup> September 2020 replaces the original version published on 14<sup>th</sup> August 2020, in order to correct errors in the title and author information, and errors in Table S2 and in the sample names labelled in Fig. S2 and Fig. S14-S16.

**Synthesis of polyoxometalate encapsulated in UiO-66(Zr) with hierarchical porosity and double active sites for oxidation desulfurization of fuel oil at room temperature**

Gan Ye<sup>a</sup>, Liangliang Hu<sup>a,b</sup>, Yulong Gu<sup>a</sup>, Christine Lancelot<sup>b</sup>, Alain Rives<sup>b</sup>, Carole Lamonier<sup>b</sup>, Nicolas Nuns,<sup>c</sup> Maya Marinova<sup>c</sup>, Wei Xu<sup>d</sup>, Yinyong Sun<sup>a,\*</sup>

*<sup>a</sup>MIIT Key Laboratory of Critical Materials Technology for New Energy Conversion and Storage, School of Chemistry and Chemical Engineering, Harbin Institute of Technology, Harbin, 150001, China*

*<sup>b</sup>Univ. Lille - UMR 8181 CNRS, Centrale Lille, ENSCL, Univ. Artois- UCCS - Unité de Catalyse et de Chimie du Solide, F-59000 Lille, France*

*<sup>c</sup>Univ. Lille, CNRS, INRA, Centrale Lille, Univ. Artois, FR 2638 - IMEC - Institut MichelEug`ene Chevreul, F-59000 Lille, France*

*<sup>d</sup>State Key Lab of Inorganic Synthesis and Preparative Chemistry, College of Chemistry, Jilin University, Changchun, 130012, China*

\*To whom correspondence should be addressed.

Tel: 86 451 86413708

## 1. The procedure of control experiments for ODS

### 1.1. Pure PW as homogeneous catalyst

A certain amount of DBT was dissolved in *n*-octane (with a concentration of 1000 ppmw of sulfur from DBT) to act as model fuel. The reaction was performed under air in a closed 40 mL dram vial with a vigorous magnetic stirrer (1000 rpm) at room temperature. In a standard run, the Pure PW (10 mg) was added to model fuel (10 g) and acetonitrile (10 g), and the resulting mixture was stirred for 10 min at room temperature. The catalytic reaction process is initiated by addition of hydrogen peroxide (H<sub>2</sub>O<sub>2</sub>, 30 wt. %) as oxidant with an O/S molar ratio of 6:1. The liquid in *n*-octane were withdrawn at regular intervals and analyzed by gas chromatography on an Agilent 7890A GC with an FID detector using a 30 m packed HP5 column.

### 1.2. UiO-66(Zr)-green as catalyst

The similar procedure to Pure PW was adopted except that 50 mg UiO-66(Zr)-green replaced the pure PW as catalyst.

### 1.3. PW+UiO-66-green as catalyst

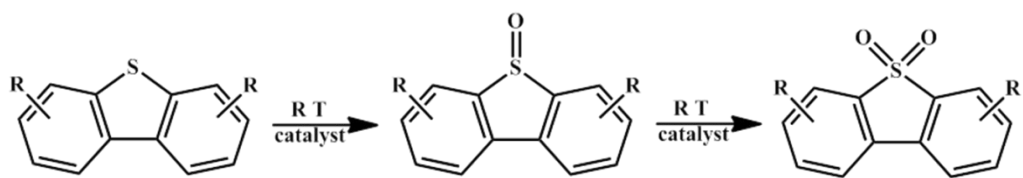
The similar procedure to Pure PW was adopted except that a physical mixture of 10 mg PW and 40 mg UiO-66(Zr)-green replaced the pure PW as catalyst.

### 1.4. PW+UiO-66-solvent as catalyst

The similar procedure to Pure PW was adopted except that a physical mixture of 10 mg PW and 40 mg UiO-66(Zr)-solvent replaced the pure PW as catalyst.

### 1.5. PW/UiO-66-solvent as catalyst

The similar procedure to Pure PW was adopted except that a physical mixture of 50 mg PW/UiO-66(Zr)-solvent replaced the pure PW as catalyst.



**Scheme S1** Reaction pathway about the ODS reaction of DBT or 4,6-DMDBT.

**Table S1** The surface chemical composition in various samples.

Catalyst	nW/nZr	nC/nZr	nC <sub>(288.8)</sub> /nZr
UiO-66(Zr)-green	0	11.7	1
PW+ UiO-66(Zr)-green	0.03	10.8	1
PW/UiO-66(Zr)-solvent	0.12	20.2	1.6
PW/UiO-66(Zr)-green	0.3	9.7	1.2

**Table S2** Comparison of catalytic activities over several POM/MOFs in ODS of DBT.

Solid carrier <sup>a</sup>	Active species and content (wt %)	Dosage of catalyst (mg)	Sulfur content (ppmw)	Temp. (°C)	Time (min)	Converted (wt %)	TOF (h <sup>-1</sup> ) <sup>c</sup>	Ref.
MIL-101(Al)-NH <sub>2</sub>	PW <sub>11</sub> Zn (15.84)	86.3	500	50	360	96.6	0.4	1
MIL-101(Cr)	Tb(PW <sub>11</sub> ) <sub>2</sub> (27)	61	500	50	180	99	0.9	2
MIL-101(Al)-NH <sub>2</sub>	Eu(PW <sub>11</sub> ) <sub>2</sub> (2.37)	12.2	500	70	120	100	2.8	3
HKUST-1	PMo <sub>12</sub> (–)	60	100	65	180	99	–	4
MIL-101(Al)-NH <sub>2</sub>	PW <sub>12</sub> (38.9)	21	500	60	240	100	2.9	5
MIL-101(Cr)	PW <sub>12</sub> (48.9)	26	500	50	60	100	1.9	6
MIL-101(Cr)	PW <sub>9</sub> (14.5)	46	500	50	60	99	2.8	7
MIL-101(Cr)	PW <sub>12</sub> (50)	75	910	45	180	91	4.7	8
MIL-101(Cr)	PW <sub>12</sub> (12)	50	500	60	120	84.1	11.3	9
MIL-101(Cr)-NH <sub>2</sub>	PW <sub>12</sub> (36.3)	50	950	50	60	100	15.9	10
ZIF-8(Zn)	PW <sub>12</sub> (10)	30	950	70	60	13	5.0	11
UiO-66(Zr)	PW <sub>12</sub> (10)	30	950	70	60	73	28.1	11
MIL-100(Fe)	PW <sub>12</sub> (16)	30	950	70	60	100	24.0	11
UiO-67(Zr)	PW <sub>12</sub> (28)	50	1000	70	60	99.7	21.5	12
TMU-17-NH <sub>2</sub>	PW <sub>12</sub> (20)	20	500	US <sup>b</sup>	15	98	38.4	13
MOF-808(Zr)	PW <sub>12</sub> (42)	12	1000	60	30	100	48.6	14
UiO-66(Zr)-solvent	PW <sub>12</sub> (14.1)	50	1000	25	60	68.9	87.8	This work
UiO-66(Zr)-green	PW <sub>12</sub> (14.7)	50	1000	25	25	99.7	293.0	This work

<sup>a</sup> All catalysts used H<sub>2</sub>O<sub>2</sub> as oxidant;

<sup>b</sup> Ultrasound irradiation power (W) 37 kHz frequency;

<sup>c</sup> TOF = (mole number of converted DBT) / (mole of active species content in catalyst × reaction time (h)).

**Table S3** Reaction rate constants were obtained at different temperatures in ODS of DBT.

Temperature (°C)	Reaction rate constant kapp (min <sup>-1</sup> )	R <sup>2</sup>
25	0.21954	0.995
40	0.33044	0.985
50	0.4606	0.973

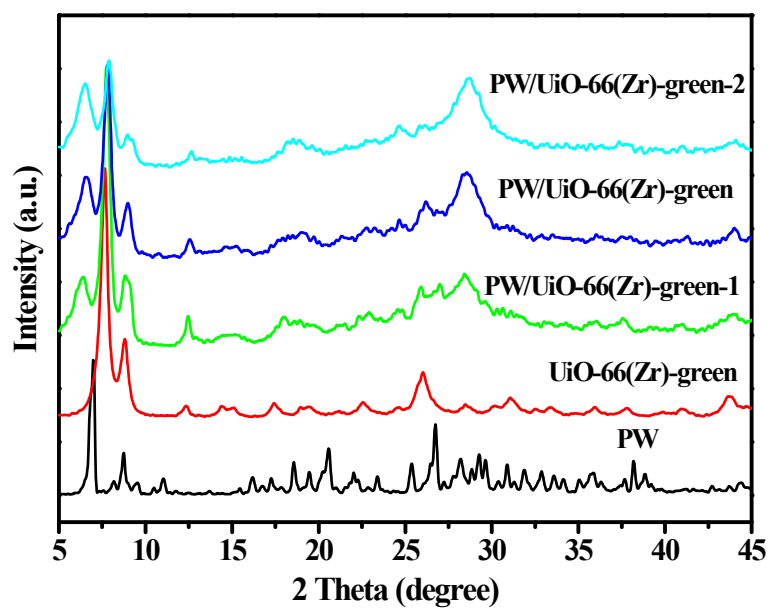


Figure S1 XRD patterns of various samples.

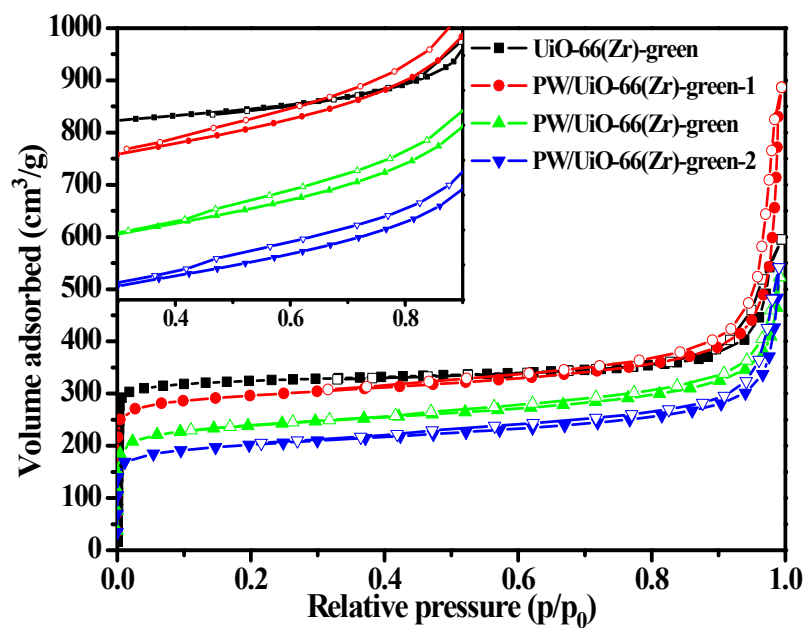
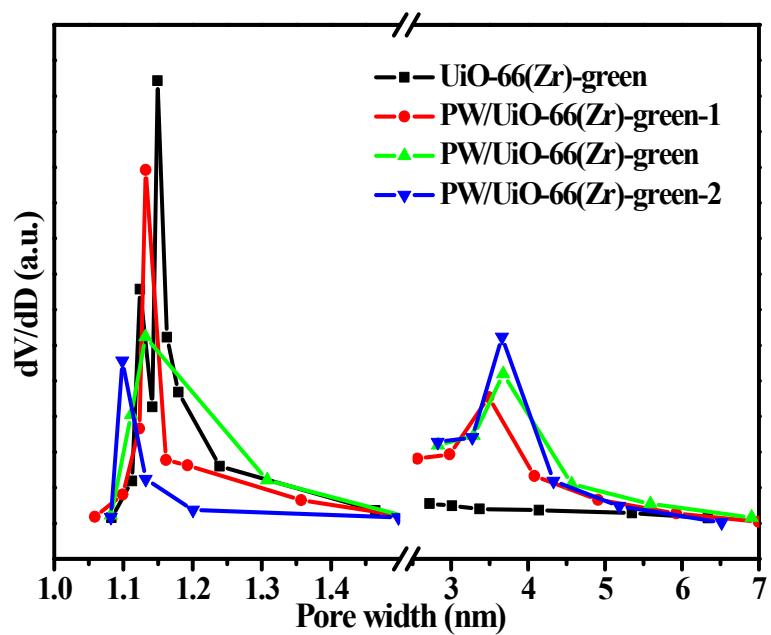
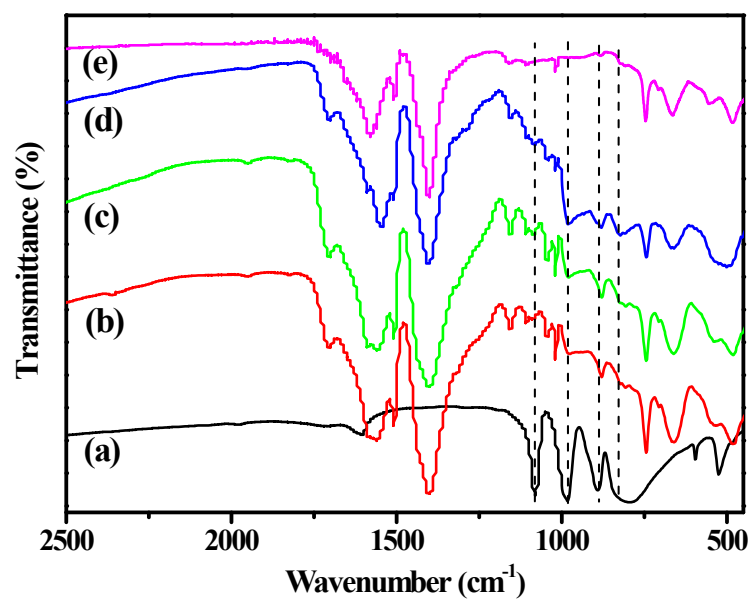


Figure S2 N<sub>2</sub> sorption isotherms with local enlargement (insert) of different samples.



**Figure S3** The micropore and mesopore distribution curves of different samples.





**Figure S4** FT-IR spectra of (a) PW, (b) PW/UiO-66(Zr)-green-1, (c) PW/UiO-66(Zr)-green, (d) PW/UiO-66(Zr)-green-2, and (e) UiO-66(Zr)-green.

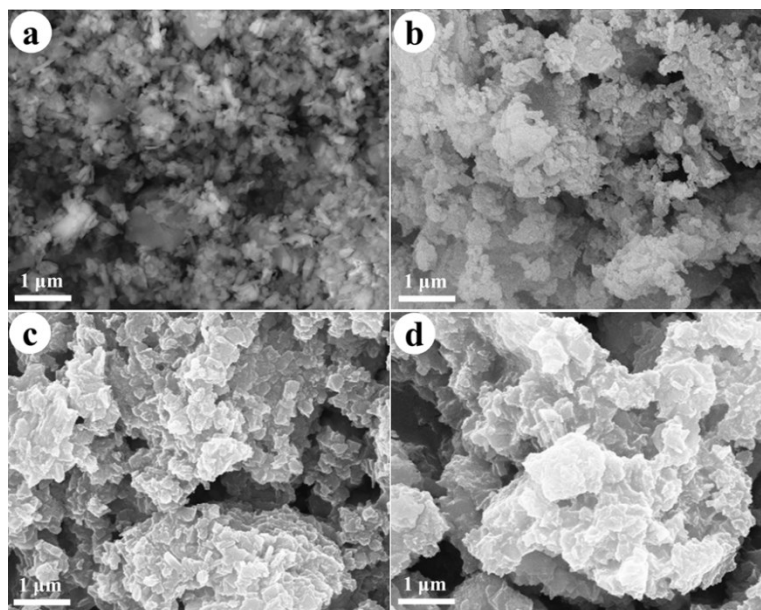


**Figure S5** SEM images of (a) UiO-66(Zr)-green, (b) PW/UiO-66(Zr)-green-1, (c) PW/UiO-66(Zr)-green, (d) PW/UiO-66(Zr)-green-2.

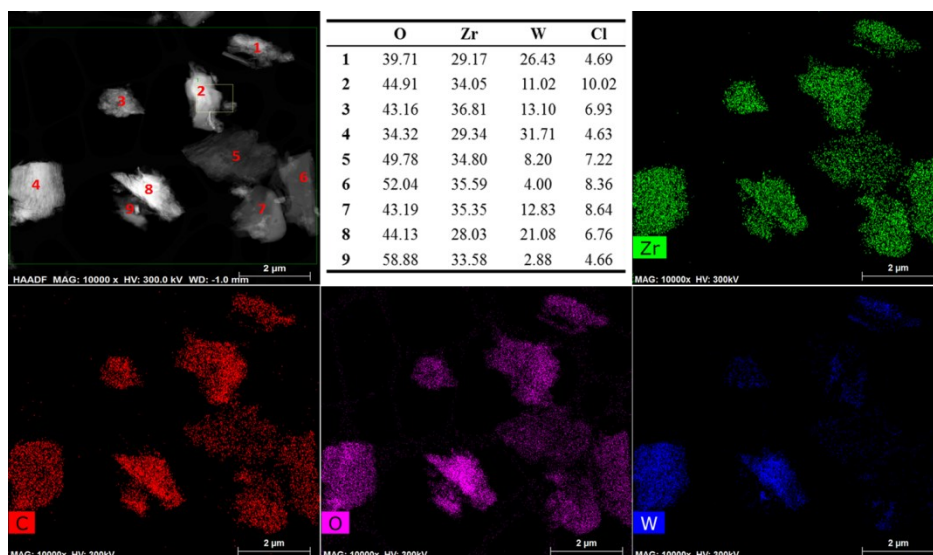


**Figure S6** HAADF images and STEM-EDS element maps of PW/UiO-66(Zr)-green together with the relative concentrations in at %.

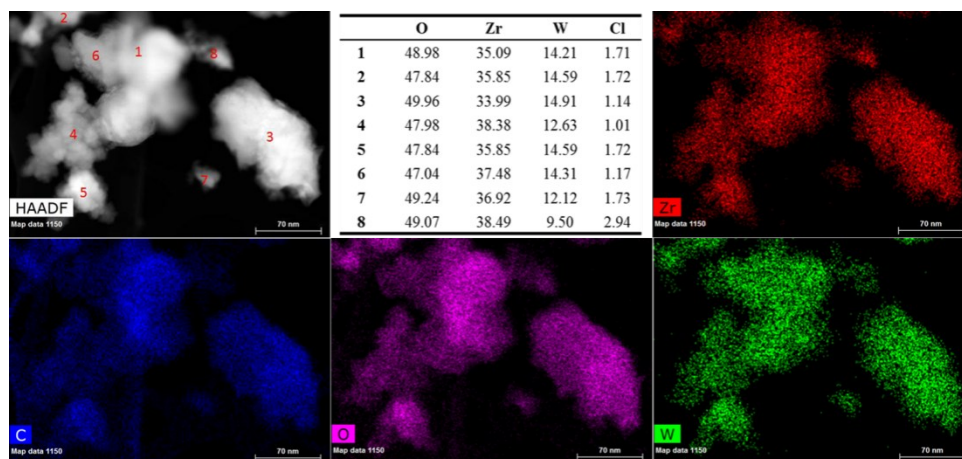


**Figure S7** HAADF images and STEM-EDS element maps of PW/UiO-66(Zr)-solvent together with relative concentration in at %.

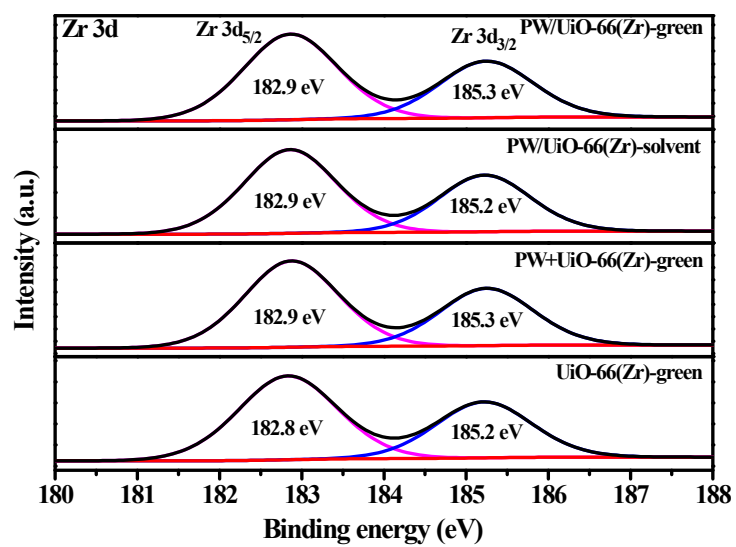


**Figure S8** XPS spectra of various samples: Zr 3d.

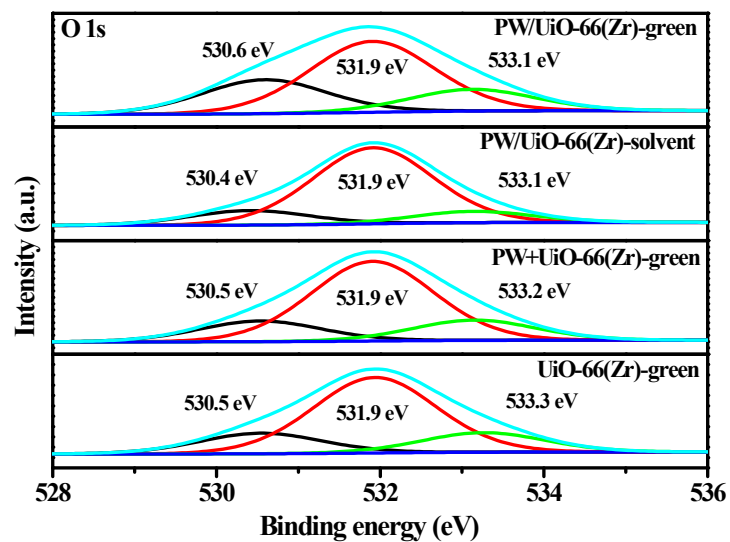


Figure S9 XPS spectra of various samples: O 1s.

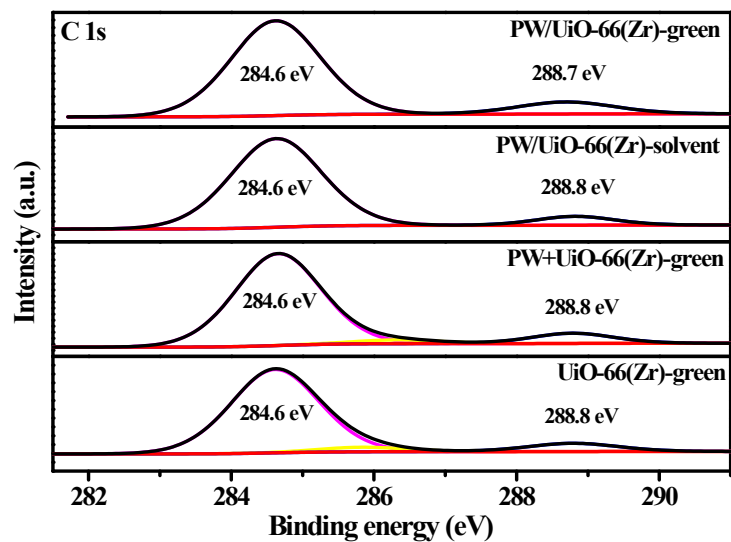
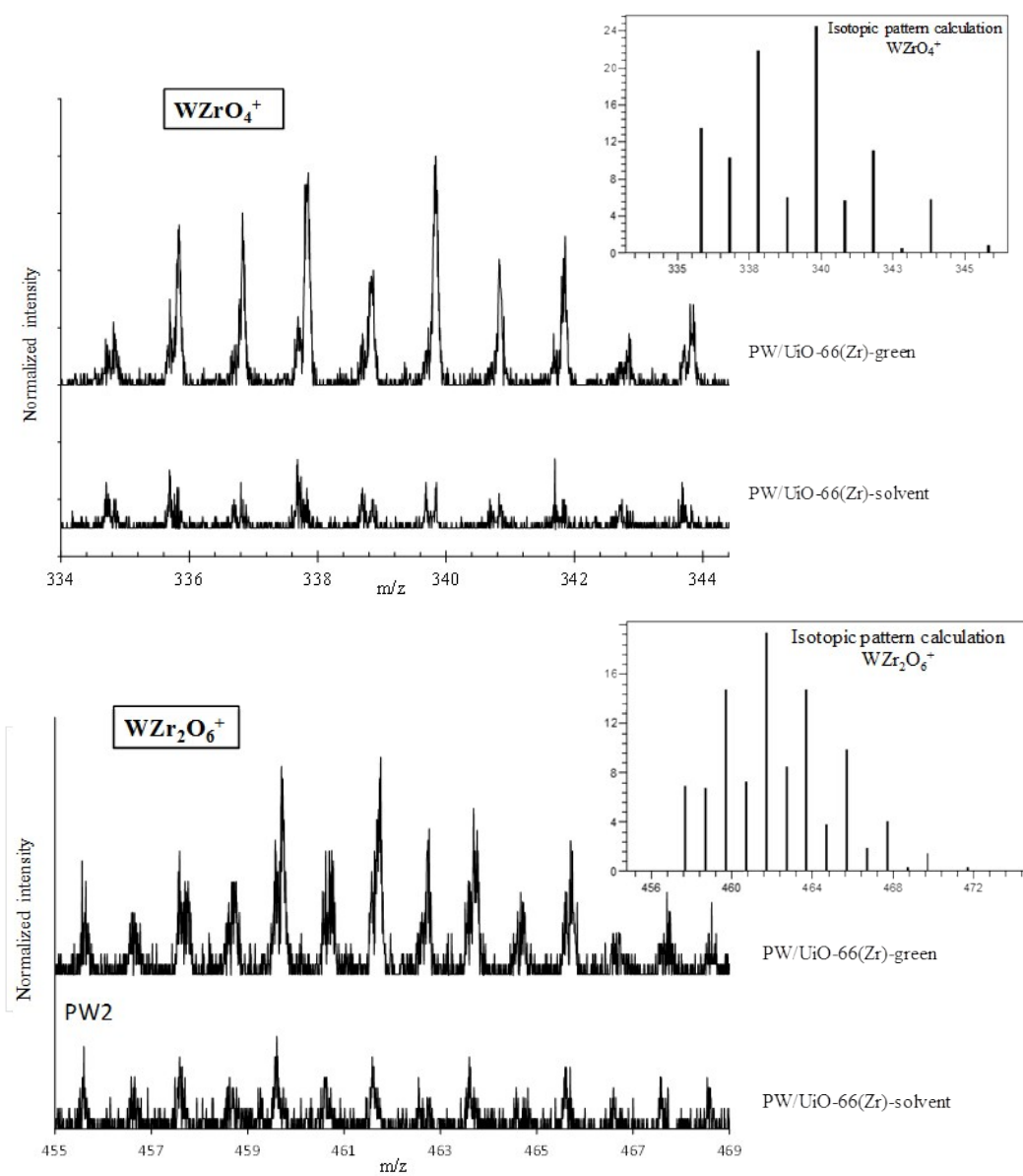
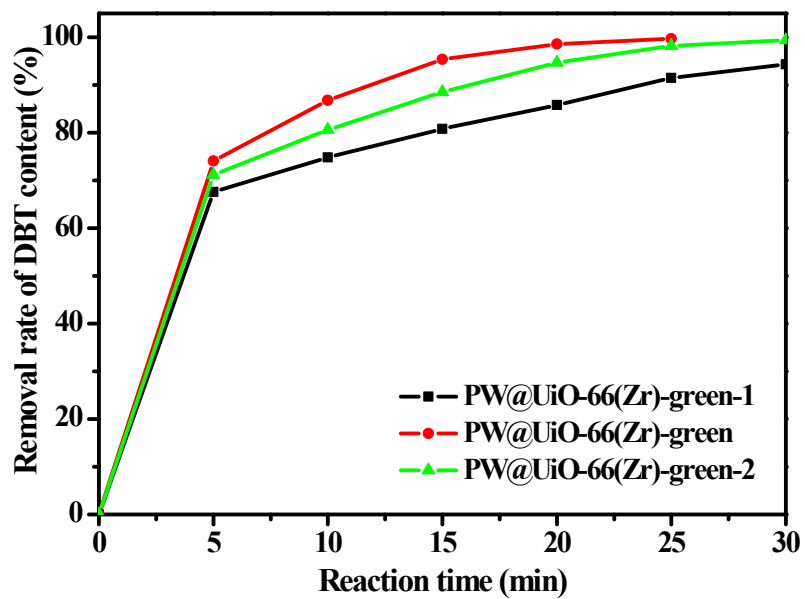


Figure S10 XPS spectra of various samples: C 1s.



**Figure S11** Identification of  $WZrO_4^+$  and  $WZr_2O_6^+$  fragments on  $PW/UiO-66(Zr)$ -green and  $PW/UiO-66(Zr)$ -solvent and simulation of their isotopic patterns.





**Figure S12** Removal content of DBT with reaction time over different catalysts at room temperature.

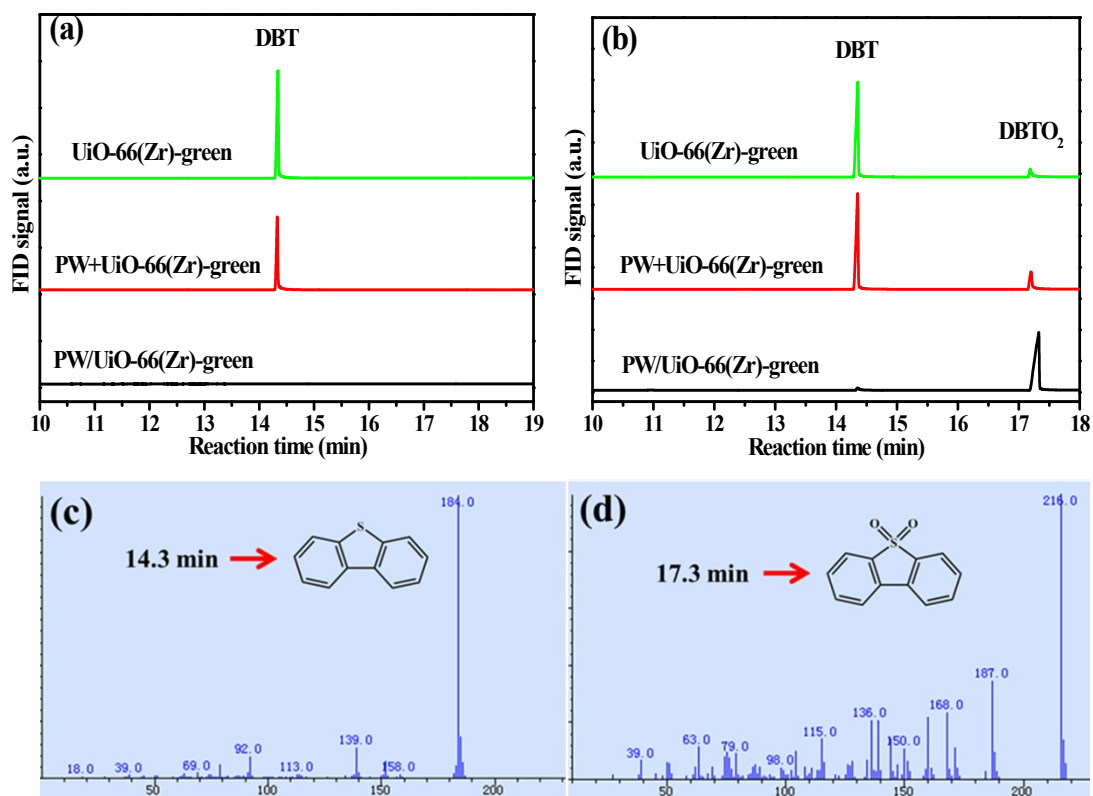


**Figure S13** GC-FID chromatograms of (a) model fuel, (b) acetonitrile phase after reaction over various samples and mass spectroscopy of (c) DBT, (d) DBTO<sub>2</sub> in the product.

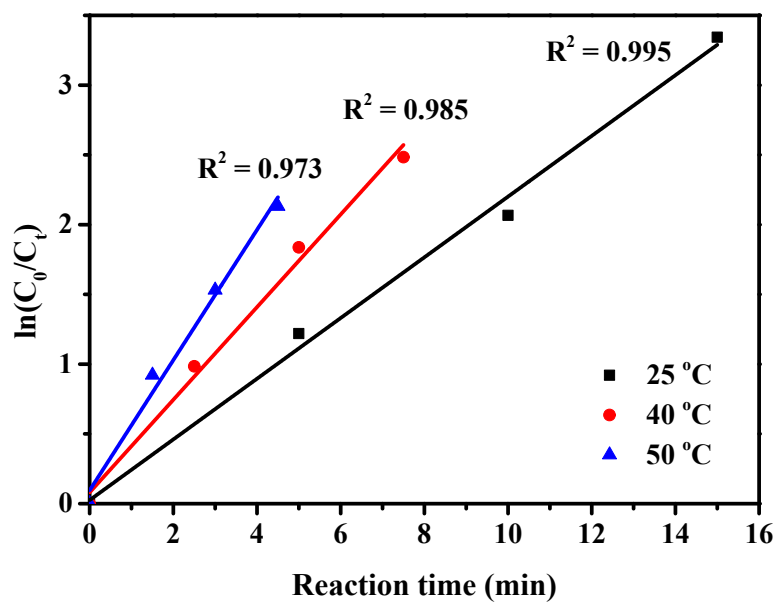


**Figure S14** Pseudo-first-order rate constants for DBT ODS reaction at different temperatures over PW/UiO-66(Zr)-green.

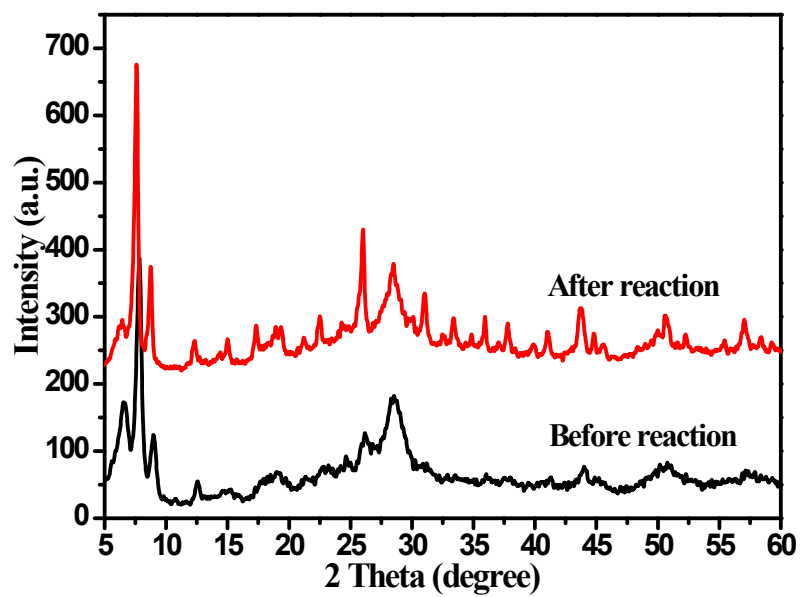
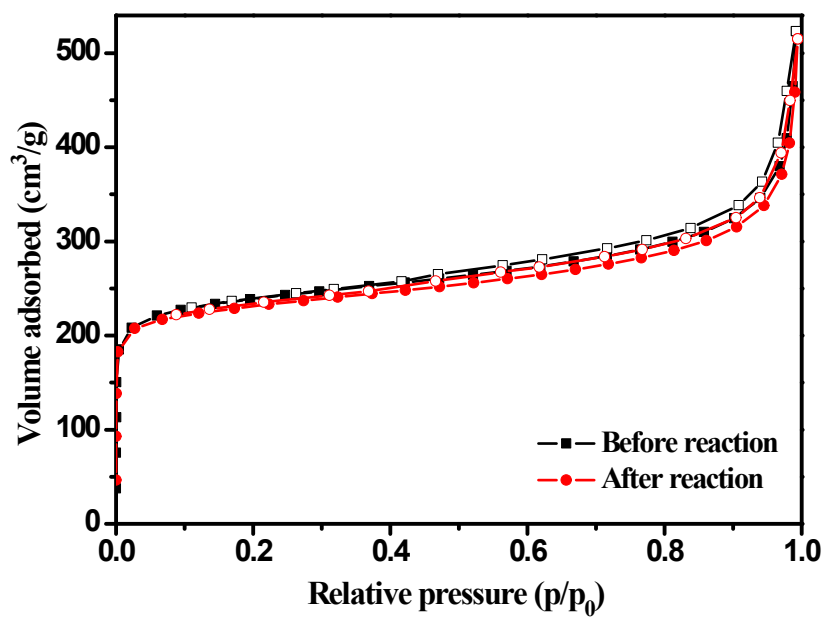


Figure S15 XRD patterns of PW/UiO-66(Zr)-green before and after reaction.



**Figure S16** N<sub>2</sub> sorption isotherms of PW/UiO-66(Zr)-green before and after reaction.

## References

- [1] D. Julião, A. C. Gomes, M. Pillinger, R. Valença, J. C. Ribeiro, B. de Castro, I. S. Gonçalves, L. C. Silva and S. S. Balula, *Eur. J. Inorg. Chem.*, 2016, **2106**, 5114-5122.
- [2] S. Ribeiro, C. M. Granadeiro, P. Silva, F. A. Almeida Paz, F. F. de Biani, L. Cunha-Silva and S. S. Balula, *Catal. Sci. Technol.*, 2013, **3**, 2404-2414.
- [3] C. M. Granadeiro, L. S. Nogueira, D. Julião, F. Mirante, D. Ananias, S. S. Balula and L. Cunha-Silva, *Catal. Sci. Technol.*, 2016, **6**, 1515-1522.
- [4] Rafiee, E. and Nobakht, N. *J. Mol. Catal. A: Chem.*, 2015, **398**, 17-25.
- [5] L. W. Zhang, S. H. Wu, Y. Liu, F. F. Wang, X. Hand and H. Y. Shang, *Appl. Organometal. Chem.*, 2016, **30**, 684-690.
- [6] S. Ribeiro, A. D. S. Barbosa, A. C. Gomes, M. Pillinger, I. S. Gonçalves, L. Cunha-Silva and S. S. Balula, *Fuel Process. Technol.*, 2013, **116**, 350-357.
- [7] C. M. Granadeiro, A. D. S. Barbosa, S. Ribeiro, I. C. M. S. Santos, B. Castro de, L. Cunha-Silva and S. S. Balula, *Catal. Sci. Technol.*, 2014, **4**, 1416-1425.
- [8] X. F. Hu, Y. K. Lu, F. N. Dai, C. G. Liu and Y. Q. Liu, *Micropor. Mesopor. Mater.*, 2013, **170**, 36-44.
- [9] M. Sun, W. C. Chen, L. Zhao, X. L. Wang and Z. M. Su, *Inorg. Chem. Commun.*, 2018, **87**, 30-35.
- [10] X. S. Wang, Y. B. Huang, Z. J. Lin and R. Cao, *Dalton Trans.*, 2014, **43**, 11950-11958.
- [11] X. S. Wang, L. Li, J. Liang, Y. B. Huang and R. Cao, *ChemCatChem*, 2017, **9**, 971-979.
- [12] Y. L. Peng, J. Y. Liu, H. F. Zhang, D. Luo and D. Li, *Inorg. Chem. Front.*, 2018, **5**, 1563-1569.
- [13] A. Afzalnia, A. Mirzaie, A. Nikseresht and T. Musabeygi, *Ultrason. Sonochem.*, 2017, **34**, 713-720.
- [14] Z. J. Lin, H. Q. Zheng, J. Chen, W. E. Zhuang, Y. X. Lin, J. W. Su, Y. B. Huang and R. Cao, *Inorg. Chem.*, 2018, **57**, 13009-13019.